J. Biochem. **135**, 17–24 (2004)
DOI: 10.1093/jb/mvh002

Mass Spectrometry on Segment-Specific Hydrogen Exchange of Dihydrofolate Reductase

Tatsuya Yamamoto, Shunsuke Izumi and Kunihiko Gekko*

Department of Mathematical and Life Sciences, Graduate School of Science, Hiroshima University, Higashi-Hiroshima 739-8526

Received September 24, 2003; accepted October 23, 2003

To address the effects of local structures on structural fluctuations of *Escherichia coli* dihydrofolate reductase (DHFR), the backbone-fluctuation map was determined by matrix-assisted laser desorption/ionization mass spectrometry (MALDI-MS) coupled with H/D exchange and pepsin digestion. H/D exchange kinetics was examined at 15°C with 18 identified digestion fragments covering almost the entire amino acid sequence of DHFR. These fragments exhibited significant variations in the first-order rate constant of proton exchange, k_{ex} (0.47–0.71 min^{-1}), the fraction of deuterium incorporation at the initial stage, D_0 (0.20–0.60), the fraction of deuterium incorporation at infinite time, D_∞ (0.75–0.97), and the number of protons protected from exchange, P (0.4–4.7), relative to the corresponding values for the whole DHFR molecule (k_{ex} = 0.51 min^{-1}, D_0 = 0.41, D_∞ = 0.85, and P = 20.7). H/D exchange was very fast in the fragment comprising residues 5–28 (Met20 loop), which participates in substrate uptake, and reasonably fast in disordered and hydrophobic fragments, but slow in β-strand-rich fragments. These results indicate that the local structures contribute differently to the fluctuation of the DHFR molecule, and that mass spectrometry coupled with H/D exchange and protease digestion is a useful tool for detecting segment-dependent protein fluctuation.

Key words: dihydrofolate reductase, hydrogen/deuterium exchange, mass spectrometry, protease digestion, structural fluctuation.

Abbreviations: DHFR, dihydrofolate reductase; ESI, electrospray ionization; MALDI, matrix-assisted laser desorption/ionization; MS, mass spectrometry; MS/MS, tandem mass spectrometry; TOF, time of flight; QIT, quadrupole ion trap.

Enzymatic function is intimately related to fluctuations of a protein to adopt conformations suitable for binding a substrate and a cofactor. However, it remains unclear how the local structures are linked to fluctuations of the whole protein molecule. Dihydrofolate reductase (DHFR) from *Escherichia coli* is a typical system for studying the structure–fluctuation–function relationships of enzymes. It is a monomeric protein consisting of 159 amino acids with no disulfide bonds, and catalyzes the NADPH-linked reduction of dihydrofolate to tetrahydrofolate. The movie constructed by Sawaya and Kraut (*1*), based on X-ray structures and ligand binding kinetics, demonstrates how the DHFR molecule actively and cooperatively fluctuates to accommodate the coenzyme and substrate. A high-pressure NMR study has revealed the existence of active-site hinge motion, including the Met20 loop in solution, that might be directly relevant to function (*2*). In our previous studies (*3–5*) we found that site-directed mutagenesis at Gly67, Gly121, and Ala145 in three independent loops significantly influences the stability and function of this enzyme, even though these positions are far separated from the catalytic residue, Asp27. These observations indicate that DHFR can assume highly fluctuating conformations in solution, a detailed knowledge of which may be crucial to understanding reaction mechanisms.

Protein dynamics has been investigated using various techniques to detect their magnitude and time scale (*6–9*), including the B-factor of X-ray crystallography, order parameter of NMR, compressibility, hydrogen/deuterium (H/D) exchange kinetics, and fluorescence relaxation time. Among these techniques, H/D exchange is a novel means of determining concomitantly the exchange rate and number of protons (*10*, *11*). H/D exchange has been monitored mainly by infrared spectroscopy and NMR (*12–14*), but recent developments in electrospray ionization mass spectrometry (ESI-MS) and matrix-assisted laser desorption/ionization mass spectrometry (MALDI-MS) have opened a new field in the study of H/D exchange in proteins, because the number of exchangeable protons can be determined rapidly and with an accuracy of 1.006 Da using only a small sample. Zhang and Smith were the first to show the usefulness of mass spectrometry coupled with pepsin digestion in the study of H/D exchange in proteins (*15*). This technique has been applied to studies of protein–inhibitor interactions (*16*) and conformational changes (*17–19*).

In the present study, we studied the H/D exchange kinetics of apo-type DHFR by MALDI-TOF (time of flight)-MS coupled with pepsin digestion in order to elucidate the backbone-fluctuation map of this enzyme. This technique has the advantage that the masses of all the

*To whom correspondence should be addressed. Fax: +81-824-24-7387; E-mail: gekko@sci.hiroshima-u.ac.jp

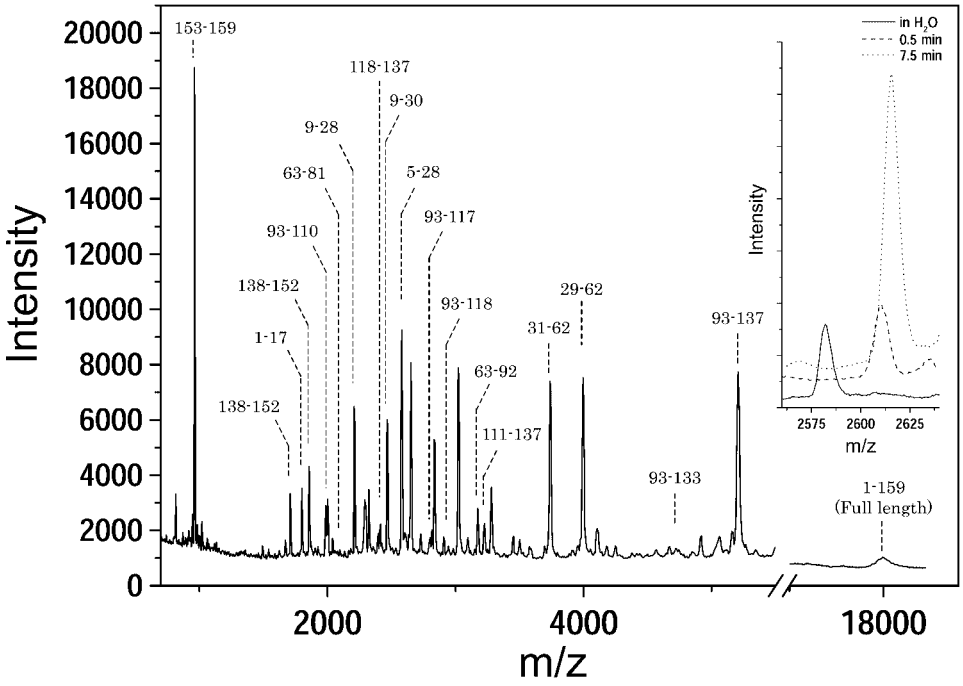

Fig. 1. **MALDI-TOF-MS spectrum of DHFR digested by pepsin.** The numbers labeling each peak correspond to the amino acid residues comprising the fragments. Inset shows the H/D exchange profile at different exchange times for fragment 5–28.

digestion fragments appear simultaneously on one spectrum, leading to a more accurate comparison of H/D exchange kinetics among the fragments. The effects of local structures on the fluctuation of the DHFR molecule are discussed on the basis of the H/D exchange kinetics parameters obtained for the fragments.

MATERIALS AND METHODS

Materials—All DHFR genes were prepared with overexpression plasmid pTP64-1 (5.3 kb) (*20*). The DHFR protein obtained from *E. coli* strain HB101 was purified on a methotrexate-agarose affinity column, then fully dialyzed against 10 mM phosphate buffer (pH 7.0) containing 0.1 mM EDTA and 0.1 mM dithiothreitol at 4°C. For mass spectrometry, DHFR solutions were finally dialyzed against 1 mM ammonium acetate. The concentration of DHFR was determined by measuring the absorption on a spectrophotometer (JASCO V-560), using a molar extinction coefficient of 31,100 $M^{-1}\cdot cm^{-1}$ at 280 nm for wild-type DHFR (*21*). Pepsin was obtained from Sigma, and D_2O (99.9% atom D) and acetic acid-*d* (99% atom D) were purchased from EURISO-TOP and IsoTec USA, respectively. All other chemicals were of analytical grade.

Pepsin Digestion—DHFR was digested with pepsin to assign the digestion fragments before the H/D exchange experiments. Two microliters of a 0.1% pepsin solution was added to a mixture of 2 μl of 20% acetic acid and 22 μl of DHFR solution, to achieve an eight-fold molar ratio of DHFR to pepsin. Pepsin digestion was carried out for 1.5 min at pH 2.4 and 0°C.

H/D Exchange—The H/D exchange reaction of DHFR was started by mixing 300 μl of D_2O with 30 μl of 250 μM DHFR (1 mM ammonium acetate) in a 1.5 ml centrifuge tube with a cap at 15°C. The pH of the mixture was 7.1 and the atomic ratio of H to D was 1:10. At 1-min intervals after starting the H/D exchange reaction, 22 μl of the reaction mixture was taken out and quenched by adding 2 μl of 20% acetic acid with an atomic ratio of H:D = 1:10. The exchange of side-chain protons can also be completed by this acid quenching. The quench time was defined as the H/D exchange time, t. The deuterized DHFR was digested with pepsin dissolved in an H_2O/D_2O mixture (H:D = 1:10) according to the procedure described above. After pepsin digestion, a portion of the sample solution was mixed with saturated α-cyano-4-hydroxycinnamic acid (CHCA) in 50% acetonitrile involving 0.1% trifluoroacetic acid, and loaded on a MALDI sample plate at 7 Pa. Ten minutes after starting the H/D exchange, the plate was set up on MALDI-TOF-MS at 10^{-5} Pa.

To compare the H/D exchange kinetics of digestion fragments consisting of different numbers of residues, the molecular weight of each fragment, M_t, at exchange time t was normalized to the exchanged fraction of amide protons, D_t, using the following equation:

$$D_t = \frac{M_t - M_{side\ chain}^{100\%}}{M_{\infty}^{theo} - M_{side\ chain}^{100\%}} \quad (1)$$

where M_{∞}^{theo} and $M_{side\ chain}^{100\%}$ are the theoretically calculated molecular weights of each fragment and its side chains, respectively, assuming a complete exchange of protons to deuterium. D_t was determined using the centroid mass of each isotopic distribution. Since the deuterium concentration in solution is very high under the experimental conditions used (H:D = 1:10), the H/D exchange of each amide proton would follow first-order kinetics at constant pH and temperature (*11*). Therefore, the H/D exchange time course was analyzed using the following equation:

$$D_t = D_{\infty} - A\exp(-k_{ex}t) \quad (2)$$

where D_t and D_{∞} are the fractions of deuterium incorporation at exchange times t and infinity, respectively; A is the fraction of exchangeable protons that can be detected during the exchange time; and k_{ex} is the apparent first-order rate constant of the H/D exchange reaction. The

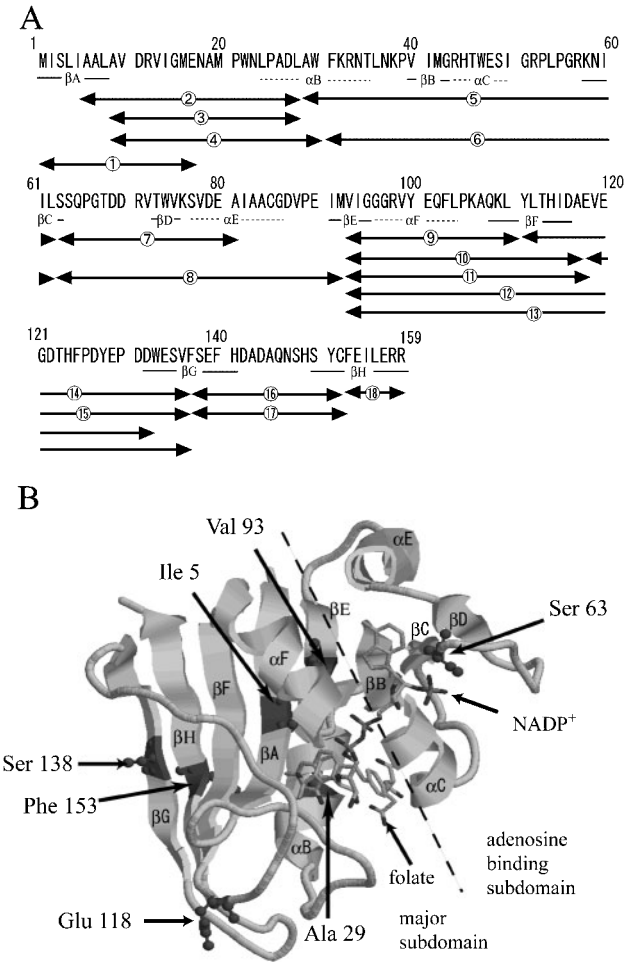

Fig. 2. **Identified pepsin-digested fragments of DHFR.** (A) Amino acid sequence of a wild-type DHFR. —, β-strand region; - - -, α-helix region. The 18 digestion fragments are indicated by arrows. (B) Three-dimensional X-ray structure of a DHFR-NAPD+-folate ternary complex (PDB: 1RA2) (*1*). Positions digested by pepsin are indicated by arrows. The dashed line indicates an assumed boundary between two subdomains.

observed k_{ex} value represents that average of all the exchange rates of the different amide protons.

Mass Spectrometry—Peptic fragments were identified and their H/D exchange examined using MALDI-TOF-MS (Voyager RP-3, Perseptive Biosystems). Proteins enclosed in CHCA crystals were ionized with an N_2 laser at 337 nm and accelerated at an accelerating voltage of 25 kV and a pulse delay time of 300 ns. Digestion fragments were identified by ESI-QIT (quadrupole ion trap)-MS/MS (tandem mass spectrometry) (LCQ, Finnigan MAT) by injecting the sample solution with a 250-μl syringe and pumping out at 5 μl·min^{-1}. Droplets including fragments were ionized at a source voltage of 4.5 kV, a capillary voltage of 10.39 V, and capillary temperature of 200°C. Low–mass fragments (~2,600 Da) were sequenced by MALDI-TOF/TOF-MS, (Ultraflex, Bruker Daltonics), and identified with NCBInr (Mascot Search, Matrix Science).

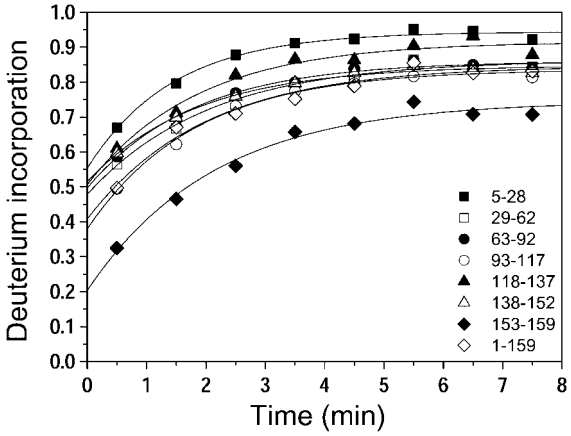

Fig. 3. **Time course of deuterium incorporation of peptic fragments of DHFR.** Lines show least-squares regressions calculated with Eq. 2.

RESULTS

Identification of Peptic Fragments of DHFR—Figure 1 shows the MALDI-TOF-MS spectra of pepsin-treated DHFR and a typical H/D exchange profile of a fragment comprising residues 5–28 (inset). The figure shows that part of the DHFR molecule remains undigested under the conditions used. Peptic fragments were assigned by sequencing by MALDI-TOF-MS/MS and ESI-QIT-MS/MS in H_2O. First, the peaks due to pepsin autolysis were eliminated and then low-mass fragments (~2,600 Da) were identified by MS/MS sequencing by MALDI-TOF/TOF-MS. Other fragments were separated from the mixtures of peptic fragments by HPLC and analyzed by off-line ESI-QIT-MS/MS (data not shown). Most peaks observed in the MS/MS spectra were assigned as b-, y-, and hydrated-y-type ions. All fragments were confirmed from the digestion-induced mass shifts of DHFR mutants, M42S, G67V, G121L, G121H, D131G, D131A, and D131R. The 18 fragments identified comprised residues 1–17, 5–28, 9–28, 9–30, 29–62, 31–62, 63–81, 63–92, 93–110, 93–117, 93–118, 93–133, 93–137, 111–137, 118–137, 138–152, 138–153, and 153–159, which cover almost the entire sequence of DHFR. The location of these fragments in the primary and three-dimensional structures of DHFR is shown in Fig. 2, together with the regions of α-helices and β-strands.

H/D Exchange of DHFR Fragments—As shown in the typical H/D exchange profile in the inset of Fig. 1, the mass peaks of all digestion fragments shift to a larger *m/z* region with the exchange from hydrogen to deuterium. The deuterium incorporations (*D*) of seven typical fragments and the whole DHFR molecule are plotted as a function of exchange time in Fig. 3. It can be expected that all side-chain protons are perfectly exchanged within this time range (less than 10 min), because the H/D exchange reaction was quenched by acetic acid-*d* in 91% deuterium oxide (pH 2.4) (*15*). It is clear that all fragments exhibit an exponential time course, and the least-squares regression lines calculated from Eq. 2 fit the data points satisfactorily. Similar results were also obtained for the other 11 fragments. The kinetics param-

Table 1. **H/D exchange kinetics parameters of peptic fragments of DHFR.**[a]

No.	Residue	M_w	M_∞^{theo}	D_∞	A	k_{ex} (min^{-1})	D_0	P
1	1–17	1,802.21	1,825.99	0.82 ± 0.02	0.45 ± 0.04	0.53 ± 0.11	0.37	2.6
2	5–28	2,581.02	2,613.95	0.94 ± 0.01	0.39 ± 0.03	0.69 ± 0.09	0.55	1.1
3	9–28	2,212.55	2,241.82	0.97 ± 0.02	0.37 ± 0.04	0.64 ± 0.15	0.60	0.4
4	9–30	2,469.84	2,501.85	0.92 ± 0.01	0.37 ± 0.02	0.71 ± 0.08	0.55	1.3
5	29–62	4,000.72	4,062.93	0.86 ± 0.02	0.38 ± 0.02	0.49 ± 0.08	0.48	3.7
6	31–62	3,743.44	3,802.90	0.86 ± 0.01	0.37 ± 0.02	0.55 ± 0.09	0.50	3.5
7	63–81	2,077.17	2,111.93	0.84 ± 0.01	0.36 ± 0.01	0.55 ± 0.04	0.47	2.5
8	63–92	3,177.48	3,224.13	0.86 ± 0.01	0.36 ± 0.02	0.56 ± 0.07	0.50	3.4
9	93–110	2,003.35	2,033.54	0.87 ± 0.01	0.42 ± 0.02	0.47 ± 0.07	0.44	1.9
10	93–117	2,817.24	2,857.49	0.84 ± 0.01	0.46 ± 0.02	0.55 ± 0.06	0.38	3.4
11	93–118	2,946.36	2,988.44	0.83 ± 0.01	0.45 ± 0.03	0.61 ± 0.08	0.38	3.7
12	93–133	4,750.15	4,813.27	0.89 ± 0.01	0.44 ± 0.01	0.48 ± 0.04	0.45	3.8
13	93–137	5,212.64	5,281.25	0.87 ± 0.01	0.43 ± 0.01	0.51 ± 0.04	0.45	4.7
14	111–137	3,227.31	3,267.56	0.92 ± 0.01	0.42 ± 0.01	0.48 ± 0.04	0.50	1.6
15	118–137	2,413.42	2,443.60	0.92 ± 0.02	0.41 ± 0.04	0.54 ± 0.12	0.51	1.3
16	138–152	1,710.69	1,739.05	0.85 ± 0.01	0.33 ± 0.02	0.55 ± 0.07	0.51	1.9
17	138–153	1,857.87	1,887.14	0.84 ± 0.01	0.36 ± 0.02	0.53 ± 0.08	0.48	2.2
18	153–159	962.10	979.48	0.75 ± 0.02	0.54 ± 0.04	0.47 ± 0.09	0.20	1.4
19	1–159	17,999.2	18,250.7	0.85 ± 0.02	0.44 ± 0.04	0.51 ± 0.11	0.41	20.7
20	82–92	1,100.31	1,112.20	0.90 ± 0.03	0.36 ± 0.05	0.57 ± 0.20	0.54	0.8
21	110–117	813.90	823.96	0.77 ± 0.02	0.55 ± 0.05	0.74 ± 0.14	0.22	1.2
22	111–118	813.90	823.96	0.97 ± 0.07	0.47 ± 0.07	0.35 ± 0.17	0.50	0.2

[a] M_w, the molecular weight of fragments digested by pepsin in H_2O; M_∞^{theo}, the molecular weight calculated for the maximum deuterium incorporation in D_2O; D_0, D_∞, deuterium incorporations at $t = 0$ and $t = \infty$, respectively; P, the number of protons remaining unexchanged at $t = \infty$; k_{ex}, the apparent first-order rate constant of the H/D exchange reaction. A is defined as $A = (D_\infty - D_0)$. Kinetics parameters for three virtual fragments (No. 20–22) were calculated from the mass difference between the two parent fragments (see text).

eters calculated (D_∞, A, and k_{ex}) are listed in Table 1, together with the fraction of deuterium incorporation at $t = 0$, which is defined as D_0 (= $D_\infty - A$). The numbers of amide protons, P, protected from deuterium exchange at $t = \infty$ are listed in the last column of Table 1. The molecular weight, M_w, of each fragment in H_2O and the theoretical molecular weight at maximum deuterium incorporation, M_∞^{theo}, at an H/D ratio of 1:10 are listed in the second and third columns of Table 1, respectively.

The H/D exchange kinetics parameters for three virtual peptides (81–92, 110–117, and 111–118), which were not identified as digestion fragments, were analyzed by adding the mass of D_2O to the mass difference between the two fragments involving the respective peptides: fragments 63–81 and 63–92 for peptide 81–92, fragments 93–110 and 93–117 for peptide 110–117, and fragments 111–137 and 118–137 for peptide 111–118. The residue numbers of the virtual fragments were assigned taking the number of all amide protons and the position of the terminal amide protons in the fragment into consideration. The estimated values of D_∞, A, and k_{ex} for these three virtual fragments are also listed in Table 1.

DISCUSSION

H/D Exchange of a Whole DHFR Molecule—The H/D exchange kinetics of a protein has been explained by the following local-unfolding model (*10*, *11*):

$$\mathrm{N(H)} \underset{k_f}{\overset{k_u}{\rightleftarrows}} \mathrm{O(H)} \xrightarrow{k_c} \mathrm{O(D)} \qquad (3)$$

where 'N' represents the "folded" state of a protein; 'O' is a partially unfolded "open" state in which the exchangeable protons are exposed to the solvent; k_u, k_f, and k_c are the rate constants for each process; and 'H' and 'D' represent the hydrogen and deuterium forms of the protein, respectively. When $k_c > k_f$, the observed rate of exchange, k_{ex}, is determined by the rate of opening of the protein structure, k_u (EX_1 mechanism). If $k_c < k_f$, the observed rate of exchange is $(k_u/k_f)k_c$, and then k_{ex} is proportional to the equilibrium constant for the local unfolding process (EX_2 mechanism). In general, the H/D exchange of proteins follows the EX_2 mechanism under most conditions, and the EX_1 mechanism is observed only under conditions – such as low or high pH – where hydrogen exchange is intrinsically very rapid and no longer rate-limiting (*10*, *14*).

The H/D exchange of a small protein may occur through simultaneous local- and global-unfolding processes. These processes can be distinguished by the activation free energy for H/D exchange (large for global unfolding and small for local unfolding). To determine whether H/D exchange of a whole DHFR molecule follows the local-unfolding model, we estimated the rate of exchange (k_{ex}) for global unfolding from the equation $k_{ex}=(k_u/k_f)k_c$ using the free energy for overall unfolding by urea, 26.5 kJ·mol^{-1}, at 15°C (*22*). In this calculation, k_c was assumed to be 879.4 min^{-1}, as determined for a model peptide (poly-D,L-alanine) at pH 5–8 (*23*). k_{ex} was estimated at 0.013 min^{-1}, which corresponds to the activation free energy of 10.4 kJ·mol^{-1}. The experimentally observed k_{ex} (0.51 min^{-1}) corresponds to the activation free energy of 1.6 kJ·mol^{-1}, which is too small for exchange through glo-

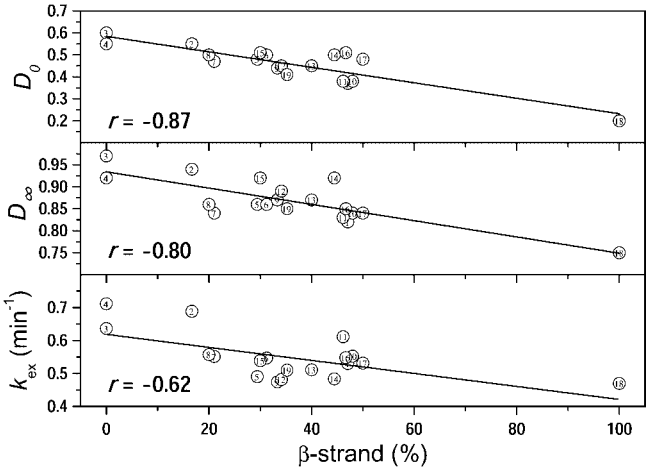

Fig. 4. **Plots of D_0, D_∞, and k_{ex} against β-strand content in peptic fragments of DHFR.** The numbers on the data points correspond to those for the fragments listed in Table 1 and Fig. 2. Lines were obtained by least-squares linear regressions for all data points, with the correlation coefficient, *r*, as indicated.

bal unfolding. This comparison reveals that the H/D exchange of a whole DHFR molecule follows a local unfolding model, which is mainly due to the EX_2 mechanism under our experimental conditions (neutral pH).

From the D_0 values in Table 1, one can expect that about 41% of the amide protons of a whole DHFR molecule exchange rapidly, probably because they are mainly located on the molecular surface. On the other hand, the D_∞ and *P* values reveal that 85% of the amide protons are exchangeable, and about 21 protons remain unexchanged to deuterium at infinite exchange time. These exchange profiles clearly reflect the overall fluctuation of the protein molecule, which is averaged for the fluctuation of all the fragments.

H/D Exchange of Peptic Fragments—As shown in Table 1, peptic fragments induce significant changes in k_{ex} (0.47–0.71 min^{-1}), D_0 (0.20–0.60), and D_∞ (0.75–0.97) from the corresponding values for the whole DHFR molecule: k_{ex} = 0.51 min^{-1}, D_0 = 0.41, and D_∞ = 0.85. These results indicate characteristic differences in the local fluctuations of a DHFR molecule. As judged from the very large values of k_{ex}, D_0, and D_∞, fragments 5–28, 9–28, and 9–30 are highly fluctuating such that their amide protons are almost completely exchanged to deuterium ($P < 1.3$). Fragment 93–118, which is rich in secondary structures, exhibits small D_0 and D_∞ values. However, fragment 138–152, with small D_0 and D_∞ values, is not necessarily rich in secondary structures. As expected,

Table 2. **Correlation coefficients between H/D exchange kinetic parameters and contents of secondary structures (PDB:5DFR).**

Parameters	α-helix	β-strand	Others
D_0	0.16	–0.87	0.80
A	–0.12	0.68	–0.62
D_∞	0.12	–0.80	0.75
P	0.37	0.15	–0.46
k_{ex}	0.19	–0.62	0.52

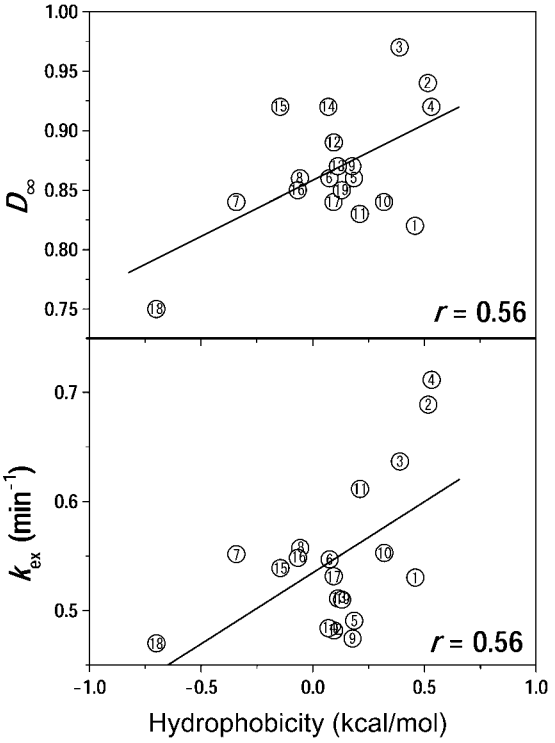

Fig. 5. **Plots of D_∞ and k_{ex} against hydrophobicity of peptic fragments of DHFR.** Lines represent the least-squares linear regressions, with the correlation coefficient, *r*, as indicated.

fragment 153–159 at the C-terminal region (βH) has a small D_0 (0.20), k_{ex} (0.47), and D_∞ (0.75).

The H/D exchange parameters of the three virtual fragments (81–92, 110–117, and 111–118) are similar to those of the respective parent fragments, but a large variation in D_∞ is observed for fragment 111–118. The parameters for fragment 110–117 differ greatly from those for fragment 111–118 despite only one shift in amino acid residues, suggesting that additional deuterium exchange occurs at terminal residues of fragment 110–117. As described above, mass spectrometry allows the detection of small differences in the fluctuation of fragments, and the H/D exchange of each fragment is affected not only by global fluctuations in a whole DHFR molecule but also by the local environment of the fragments in the tertiary structure. Therefore, it is pertinent to discuss the H/D exchange of fragments based on their structural characteristics.

Effects of Secondary Structure on H/D Exchange—It is generally known that amide protons in the secondary structure of proteins are protected from H/D exchange (*24*). If this is the case for DHFR, there should be a negative correlation between the kinetics parameters and the α-helix and β-strand contents involved in each fragment. We, therefore, examined the correlation between these factors based on the X-ray structure of DHFR (PDB: 5DFR) (*25*). As shown in Fig. 4, there was a good correlation between the kinetics parameters (D_0, D_∞, and k_{ex}) and the β-strand content of each fragment. The negative slopes for D_0, D_∞, and k_{ex}, and the positive slope for *P* (data not shown) are strong evidence that β-sheets suppress the fluctuation of the DHFR molecule. The correla-

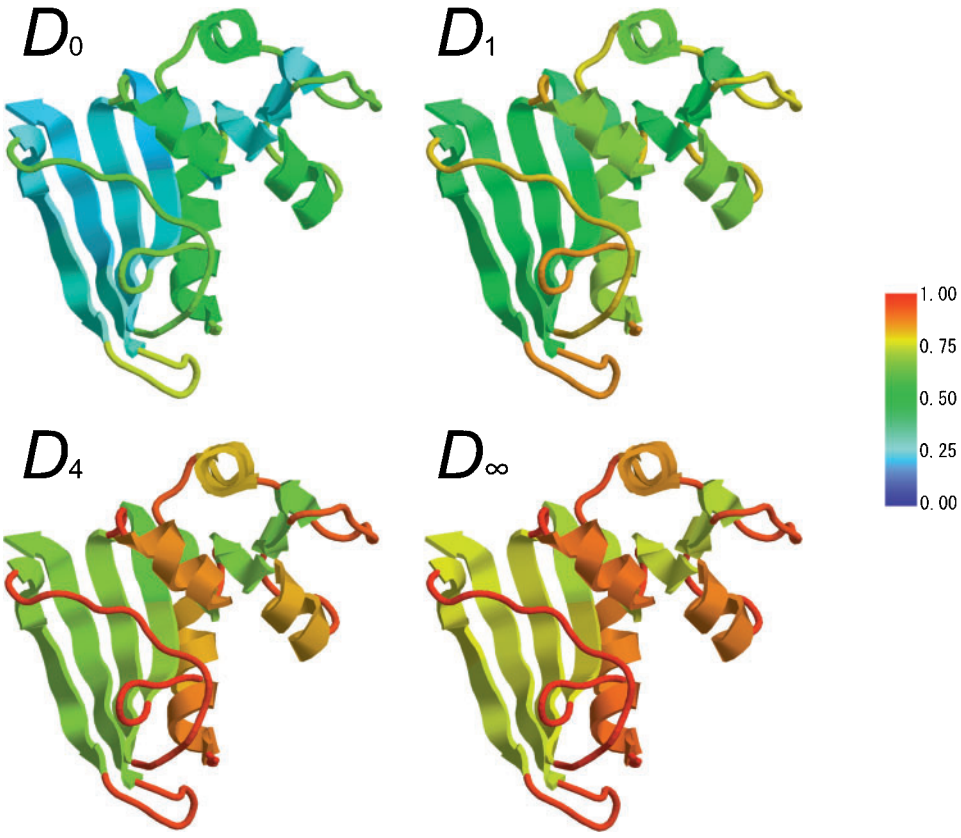

Fig. 6. **Fluctuation map of DHFR at different H/D exchange times.** The colors of the segments correspond to the proportion of deuterium incorporation trisected with H/D exchange parameters at each exchange time.

tion coefficients for the data points are listed in Table 2 together with those for the α-helix and other (disordered) structures. There are only small correlations between the α-helix content and the kinetics parameters, suggesting that the α-helix moiety does not play a dominant role in depressing fluctuations in this protein. In contrast to the data for β-strand content, the correlation coefficient with the amount of disordered structure is positive for D_0 (r = 0.80), k_{ex} (r = 0.52), and D_∞ (r = 0.75), and negative for P (r = –0.46), supporting the notion that disordered regions fluctuate sufficiently to make their amide protons susceptible to deuterium exchange. DHFR has several loops (residues 9–24, 64–72, 117–131, and 142–149) as revealed by the large B-factor in the X-ray crystal structure (*25*). The loop comprising residues 9–24 (Met20 loop) fluctuates the most and is important for the uptake of substrate and coenzyme into the binding pocket. Fragments 5–28, 9–28, and 9–30, which include the Met20 loop, consistently show very large k_{ex}, D_0, and D_∞ values (compared with fragments involving other loops), and hence amide protons in these fragments are completely exchanged to deuterium (P < 1.3) (Table 1). D_∞ has a positive correlation (r = 0.75) with mean B-factor of amide-nitrogen in each fragment calculated from the X-ray structure of DHFR (PDB: 5DFR) (*25*), suggesting that the fluctuation of each fragment in solution reflects that in crystal.

In order to clarify the contributions of α-helix, β-strand, and disordered forms to H/D exchange, D_t was decomposed into these three components by multiple regression analysis using the fractions of the α-helix (f_α), β-strand (f_β), and disordered forms (f_d) in each of 18 fragments as independent variables:

$$D_t = D_{t,\alpha} f_\alpha + D_{t,\beta} f_\beta + D_{t,d} f_d \quad (4)$$

where $D_{t,\alpha}$, $D_{t,\beta}$, and $D_{t,d}$ represent the deuterium incorporations into the α-helix, β-strand, and disordered forms at time t, respectively. Their values were calculated to be as follows: $D_{0,\alpha}$ = 0.42, $D_{0,\beta}$ = 0.14, and $D_{0,d}$ = 0.64 (multiple correlation coefficient, r^2 = 0.93); and $D_{\infty,\alpha}$ = 0.87, $D_{\infty,\beta}$ = 0.75, and $D_{\infty,d}$ = 0.97 (r^2 = 0.98). These results confirm that H/D exchange is depressed in the β-sheet, whereas the α-helix and disordered structure have high levels of deuterium incorporation.

Effects of Hydrophobicity on H/D Exchange—Hydrophobic amino acid residues are generally localized in the interior of a protein molecule to stabilize the structure by hydrophobic interactions. DHFR has three hydrophobic clusters (*26*): two in the major subdomain (a large cluster between the β-sheet and αF-helix, and a small cluster between the β-sheet and αB-helix) and one in the adenosine-binding subdomain (a small cluster consisting of Met42, Trp47, Ile61, Val72, and Trp74 between the αC-helix and β-sheet). If such hydrophobic clusters contribute to stabilize the structure, H/D exchange would be depressed in hydrophobic fragments. However, as shown in Figure 5, D_∞ and k_{ex} increase with an increase in the average hydrophobicity of peptic fragments (r = 0.56), indicating that hydrophobic residues enhance the fluctuations of DHFR. This is consistent with our findings that adiabatic compressibility (volume fluctuation) of globular proteins increases with increasing hydrophobicity (*7*).

Thus, hydrophobic residues would contribute to the production of cavities, which are a decisive factor in fluctuation, in a protein molecule via their imperfect atomic packing.

Fluctuation Map of a DHFR Molecule—To visualize the different fluctuation of the fragments in a DHFR molecule, the deuterium incorporation of each fragment at four exchange times is mapped with different colors in Fig. 6. D_t of each fragment was decomposed into three contributions of α-helix, β-strand, and disordered forms, based on the results of multiple regression analysis using Eq. 4. To cover the entire range of the primary structure, we selected seven peptic fragments: 5–28, 29–62, 63–92, 93–117, 118–137, 138–152, and 153–159. The D_t value for N-terminal residues 1–4 was assumed to be identical to that for fragment 1–17. Evidently, the helix and loop regions participating in substrate binding (Met20 loop, B-helix, αB-βB loop, C-helix, and αC-βC loop) are largely fluctuating. The βF-βG loop is also fluctuating and appears to move cooperatively with the Met20 loop, as found by Sawaya and Kraut (*1*). The fluctuation of the four helices appears to increase in the following order: F-helix > B-helix > C-helix > E-helix. It can be seen that β-strands fluctuate less than helix and disordered regions. Thus these fluctuation maps obtained from H/D exchange of the peptic fragments can reveal characteristic differences in the fluctuation of local structures, although they cannot monitor the site-specific fluctuation of a protein as obtained by the B-factor of X-ray crystallography (*25*) and the order parameter of NMR (*26*).

CONCLUDING REMARKS

The present study shows that mass spectrometry coupled with H/D exchange and protease digestion is advantageous for addressing the fluctuation map of a protein molecule. The digestion fragments of DHFR show significant differences in the H/D exchange kinetics parameters, indicating the presence of segment-dependent fluctuation. The fragments including the Met20 loop are fluctuating greatly, and the β-strands depress fluctuations of DHFR. Further insight into the structure-fluctuation-function relationship of DHFR could be obtained by mass spectrometry on H/D exchange coupled with ligand binding and mutation, investigations that are now in progress in our laboratory.

We thank Professor Tsutomu Masujima of Hiroshima University for providing MALDI-TOF-MS facilities. We thank also the Instrument Center for Chemical Analysis, Hiroshima University, for measurements of ESI double-focusing mass spectra, and the Faculty of Applied Biological Sciences, Hiroshima University, for providing ESI-QIT-MS/MS facilities.

This work was supported by a Grant-in-Aid (No. 10480159) for Scientific Research from the Ministry of Education, Science, Sports and Culture of Japan.

REFERENCES

1. Sawaya, M.R. and Kraut, J. (1997) Loop and subdomain movements in the mechanism of *Escherichia coli* dihydrofolate reductase: crystallographic evidence. *Biochemistry* **36**, 586–603
2. Kitahara, R., Sareth, S., Yamada, H., Ohmae, E., Gekko, K., and Akasaka, K. (2000) High pressure NMR reveals active-site hinge motion of folate-bound *Escherichia coli* dihydrofolate reductase. *Biochemistry* **39**, 12789–12795
3. Gekko, K., Kunori, Y., Takeuchi, H., Ichihara, S., and Kodama, M. (1994) Point mutations at glycine-121 of *Escherichia coli* dihydrofolate reductase: important roles of a flexible loop in the stability and function. *J. Biochem.* **116**, 34–41
4. Ohmae, E., Iriyama, K., Ichihara, S., and Gekko, K. (1996) Effects of point mutations at the flexible loop glycine-67 of *Escherichia coli* dihydrofolate reductase on its stability and function. *J. Biochem.* **119**, 703–710
5. Ohmae, E., Ishimura, K., Iwakura, M., and Gekko, K. (1998) Effects of point mutations at the flexible loop alanine-145 of *Escherichia coli* dihydrofolate reductase on its stability and function. *J. Biochem.* **123**, 839–846
6. Karplus, M. and McCammon, J.A. (1981) The internal dynamics of globular proteins. *CRC Crit. Rev. Biochem.* **9**, 293–349
7. Gekko, K. and Hasegawa, Y. (1986) Compressibility-structure relationship of globular proteins. *Biochemistry* **25**, 6563–6571
8. Wüthrich, K. (1990) Structure and dynamics in proteins of pharmacological interest. *Biochem. Pharmacol.* **40**, 55–62
9. Creighton, T. (1993) *Proteins: Structure and Molecular Properties*, Freeman and Company, New York
10. Hvidt, A. and Nielsen, S.O. (1966) Hydrogen exchange in proteins. *Adv. Protein Chem.* **21**, 287–386
11. Englander, S.W. and Kallenbach, N.R. (1983) Hydrogen exchange and structural dynamics of proteins and nucleic acids. *Q. Rev. Biophys.* **16**, 521–655
12. Nakanishi, M. and Tsuboi, M. (1976) Structure and fluctuation of a *Streptomyces* subtilisin inhibitor. *Biochim. Biophys. Acta* **434**, 365–376
13. Wagner, G. and Wüthrich, K. (1982) Amide proton exchange and surface conformation of the basic pancreatic trypsin inhibitor in solution. Studies with two-dimensional nuclear magnetic resonance. *J. Mol. Biol.* **160**, 343–361
14. Akasaka, K., Inoue, T., Hatano, H., and Woodward, C.K. (1985) Hydrogen exchange kinetics of core peptide protons in *Streptomyces* subtilisin inhibitor. *Biochemistry* **24**, 2973–2979
15. Zhang, Z. and Smith, D.L. (1993) Determination of amide hydrogen exchange by mass spectrometry: a new tool for protein structure elucidation. *Protein Sci.* **2**, 522–531
16. Akashi, S. and Takio, K. (2000) Characterization of the interface structure of enzyme-inhibiter complex by using hydrogen-deuterium exchange and electrospray ionization Fourier transform ion cyclotron resonance mass spectrometry. *Protein Sci.* **9**, 2497–2505
17. Babu, K.R. and Douglas, D.J. (2000) Methanol-induced conformations of myoglobin at pH 4.0. *Biochemistry* **39**, 14702–14710
18. Powell, K.D., Wales, T.E., and Fitzgerald, M.C. (2002) Thermodynamic stability measurements on multimeric proteins using a new H/D exchange- and matrix-assisted laser desorption/ionization (MALDI) mass spectrometry-based method. *Protein Sci.* **11**, 841–851
19. Englander, J.J., Del Mar, C., Li, W., Englander, S.W., Kim, J.S., Stranz, D.D., Hamuro, Y., and Woods V.L., Jr. (2003) Protein structure change studied by hydrogen-deuterium exchange, functional labeling, and mass spectrometry. *Proc. Natl Acad. Sci. USA* **100**, 7057–7062
20. Iwakura, M., Jones, B.E., Luo, J., and Matthews, C.R. (1995) A strategy for testing the suitability of cysteine replacements in dihydrofolate reductase from *Escherichia coli*. *J. Biochem.* **117**, 480–488
21. Fierke, C.A., Johnson, K.A., and Benkovic, S.J. (1987) Construction and evaluation of the kinetic scheme associated with dihydrofolate reductase from *Escherichia coli*. *Biochemistry* **26**, 4085–4092
22. Gekko, K., Yamagami, K., Kunori, Y., Ichihara, S., Kodama, M., and Iwakura, M. (1993) Effect of point mutations in a flex-

ible loop on the stability and enzymatic function *Escherichia coli* dihydrofolate reductase. *J. Biochem.* **113**, 74–80
23. Takahashi, T., Nakanishi, M., and Tsuboi, M. (1978) Hydrogen-deuterium exchange rate between a peptide group and an aqueous solvent as determined by a stopped flow ultraviolet spectrophotometry. *Bull. Chem Soc. Jpn.* **51**, 1988–1990
24. Pedersen, T.G., Thomsen, N.K., Andersen, K.V., Madsen, J.C., and Poulsen, F.M. (1993) Determination of the rate constants k_1 and k_2 of the Linderstrøm-Lang model for protein amide hydrogen exchange. A study of the individual amides in hen egg-white lysozyme. *J. Mol. Biol.* **230**, 651–660
25. Bystroff, C. and Kraut, J. (1991) Crystal structure of unliganded *Escherichia coli* dihydrofolate reductase. Ligand-induced conformational changes and cooperativity in binding. *Biochemistry* **30**, 2227–2239
26. Epstein, D.M., Benkovic, S.J., and Wright, P.E. (1995) Dynamics of the dihydrofolate reductase-folate complex: catalytic sites and regions known to undergo conformational change exhibit diverse dynamical features. *Biochemistry* **34**, 11037–11048